

Inhibition Effect of Solid Products and DC Breakdown Characteristics of the HFO1234Ze(E)–N₂–O₂ Ternary Gas Mixture

Heng Liu, Qingmin Li,* Jingrui Wang, Yuheng Jiang, and A. Manu Haddad



Cite This: *ACS Omega* 2021, 6, 23281–23292



Read Online

ACCESS |



Metrics & More

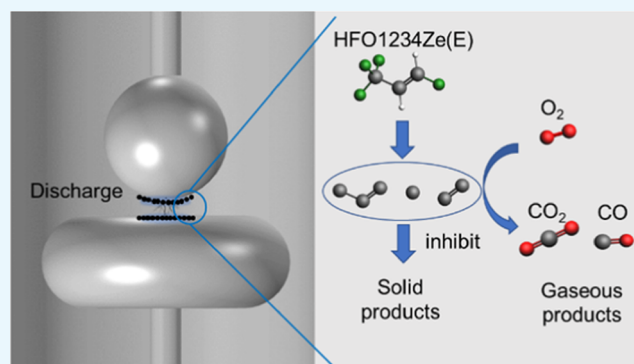


Article Recommendations



Supporting Information

ABSTRACT: HFO1234ze(E) is an environmentally friendly SF₆ substitute gas with prominent application potential. To suppress the generation of the HFO1234ze(E) solid decomposition products, which may cause great hazards to the gas–solid insulation strength, a gas mixing scheme screening method based on the reactive force field (ReaxFF) molecular dynamics (MD) simulation was innovatively proposed. The simulation results show that the inhibitory effect of O₂ on the formation of HFO1234ze(E) solid products is better than those of CO₂ and CF₄. Further study shows that when O₂ accounts for 3.33% of the gas mixture, the solid precipitate content is reduced by 48%. The experimental study shows that an O₂ content of 3.33% can inhibit the generation of solid products by more than 50%. Besides, compared with HFO1234ze(E)–N₂, the DC breakdown voltage of HFO1234ze(E)–N₂–O₂ is slightly increased, and the breakdown voltage dispersion degree and continuous breakdown voltage drop rate are decreased. This work gives a feasible solution for the suppression of HFO1234ze(E) solid decomposition products and provides an efficient method for solving similar problems of environmentally friendly insulating gas in C/F/O/N systems.



1. INTRODUCTION

Due to its high dielectric strength and excellent arc extinction performance, sulfur hexafluoride (SF₆) has been widely used in power transmission and distribution equipment, such as gas-insulated switchgear (GIS) and gas-insulated transmission line (GIL).^{1,2} However, the global warming potential (GWP) of SF₆ is 23 900 times that of CO₂ and its atmospheric lifetime is as long as 3200 years.³ SF₆ that escapes into the atmosphere will exacerbate the greenhouse effect in a quite long period of time. For environmental protection and sustainable development considerations,^{4,5} it has become an urgent need to find an environmentally friendly insulating gas to replace SF₆.

In recent years, researchers have made some progress in searching for potential SF₆ substitute gases. Some alternative candidates such as c-C₄F₈,⁶ CF₃I,⁷ C₅F₁₀O, and C₄F₇N⁸ were identified because of their strong insulation properties (equivalent to or stronger than SF₆). However, the shortcomings of the aforementioned candidate gases in terms of the greenhouse effect (c-C₄F₈), material compatibility (CF₃I), and toxicity (C₅F₁₀O and C₄F₇N) limit their wide application to some extent. Recently, HFO1234Ze(E) (referred to as hydrofluoroolefins (HFO) when it does not cause ambiguity), one of the hydrofluoroolefins family gases, shows favorable properties in replacing SF₆ in medium voltage systems.^{9,10} The GWP of this gas is very low (GWP = 6) and its ozone depletion potential is zero.¹⁰ The experimental results indicate that the breakdown voltage of HFO is 74–94% of SF₆ under

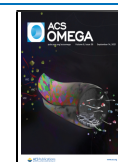
identical experimental conditions. In addition, as a refrigerant with mature applications, it is found to be nontoxic, noncarcinogenic, non-reprotoxic, and nonmutagenic.¹¹ Since the boiling point of pure HFO gas is –19 °C,¹² a buffer gas is needed to solve the problem of low-temperature liquefaction. The experimental study shows that the AC breakdown voltage of the HFO–N₂ mixture under a slightly nonuniform electric field is close to that of the SF₆–N₂ mixture.¹³

It should be noted that in experimental studies, black solid precipitates are observed to scatter near the discharge location after the discharge failure. Although some researchers have pointed out that a small amount of solid precipitates covering the electrode surface has no significant effect on the breakdown strength of the insulating gas,¹⁴ if the discharge location is near the insulator, the solid precipitates are easily dispersed on the surface of the insulating material, which may cause great hazards to the surface insulation strength. Therefore, exploring the method for suppressing the HFO solid precipitates is one of the key issues that need to be

Received: June 8, 2021

Accepted: August 20, 2021

Published: August 31, 2021



resolved before the reliable replacement of SF₆ by HFO gas. The existing literature studies have shown that the introduction of a buffer gas to adjust the gas decomposition characteristics is a potential solution to suppress the solid products. Considering that the efficiency of finding suitable buffer gases and optimal mixing schemes that can inhibit the HFO solid decomposition products through experiments is very low, it is imperative to explore a more effective research method.

After nearly 20 years of development, the molecular dynamics (MD) simulation based on the reactive force field (ReaxFF) has been very mature.¹⁵ Compared with the classical molecular force fields, ReaxFF introduces the concept of bond order (BO) to determine the covalent interaction between the atoms. By using BO, it is unnecessary to fix the connectivity of atoms so that the chemical bonds between atoms can be freely broken or formed.

In recent years, ReaxFF MD simulation has been widely used in the research of insulation gas decomposition mechanisms. Li et al. studied the decomposition characteristics of the environmentally friendly insulating gas C₅F₁₀O and analyzed the influence of the buffer gas (air) on the generation of C₃F₁₀O decomposition products.¹⁶ Zhang et al. explored the decomposition mechanism of the C₄F₇N and the C₄F₇N/CO₂ gas mixture.^{17,18} Liu et al. studied the effect of O₂ on the decomposition products of SF₆ and explained the generation mechanism of its oxygen-containing decomposition products.¹⁹ Lin et al. studied the decomposition characteristics of the HFO/N₂ mixture.¹³ In addition, ReaxFF has also been used to explore the decomposition mechanism of the hydrofluoroolefins family working fluids. Huo et al. studied the oxidation decomposition mechanism of HFO1336mzz-(Z).²⁰ Pu et al. studied the pyrolysis mechanism of HFO-1234yf (an isomer of HFO1234Ze(E)).²¹ On the basis of the above-mentioned research work, it is a feasible research approach to use ReaxFF MD simulation to guide the screening of buffer gases that could inhibit the precipitation of HFO solid decomposition products from the perspective of the micro-reaction mechanism.

In this paper, simulation and experimental research were carried out on the suppression methods of HFO solid decomposition products for the first time. This research work mainly focuses on screening suitable buffer gases to regulate the microscopic decomposition process of HFO gas, and finally, achieve the suppression of solid precipitates. To achieve this research goal, we innovatively proposed a research method for evaluating the inhibition effect of the HFO solid decomposition products by buffer gases based on ReaxFF MD simulation, which greatly improved the efficiency of the buffer gas screening process. Through ReaxFF simulation, the inhibitory effects of several candidate buffer gases on HFO solid decomposition products were simulated, and the influence mechanism of various factors on the inhibitory effects of solid products was analyzed. Furthermore, experiments were carried out to study the DC breakdown characteristics of the HFO ternary gas mixture and the suppression effect of solid products. Based on the above research, this work provides a gas mixing scheme that can effectively inhibit the HFO solid decomposition products, which could provide technical support for promoting HFO to replace SF₆ in the medium voltage equipment.

2. RESULTS AND DISCUSSION

2.1. Selection of a Buffer Gas to Inhibit HFO Solid Decomposition Products.

2.1.1. Inhibitory Effect of Different Buffer Gases on HFO Solid Precipitates.

According to the existing research results,²² the C–F, C–H, and C–C bonds in HFO molecules may break and generate many C, C₂, or C₃ particles under the action of discharge and high temperatures. When these particles recombine with each other to form clusters with a large number of carbon atoms during the cooling process, they will precipitate out of the gas reaction system and become solid products. From the above analysis, it can be seen that the fundamental way to inhibit the formation of HFO solid precipitates is to reduce the probability of the formation of carbon clusters. It can be considered from two aspects: (1) inhibit the generation of C_x particles and (2) promote the conversion of C_x particles into other gaseous products. Based on the research experience from the literature, three potential buffer gases, CO₂, O₂, and CF₄, are selected for further research in this article. Since HFO1234Ze(E) is not flammable and has no flash point according to standards, the addition of O₂ does not constitute a safety risk.

After performing 1000 ps simulation according to the settings of Section 4.1, the number of remaining HFO molecules and the number of C_x particles in the A0–A3 system are shown in Figure 1 (to reduce the influence of fluctuations (± 2) in the number of C_x particles, the average value of 900–1000 ps is taken for analysis).

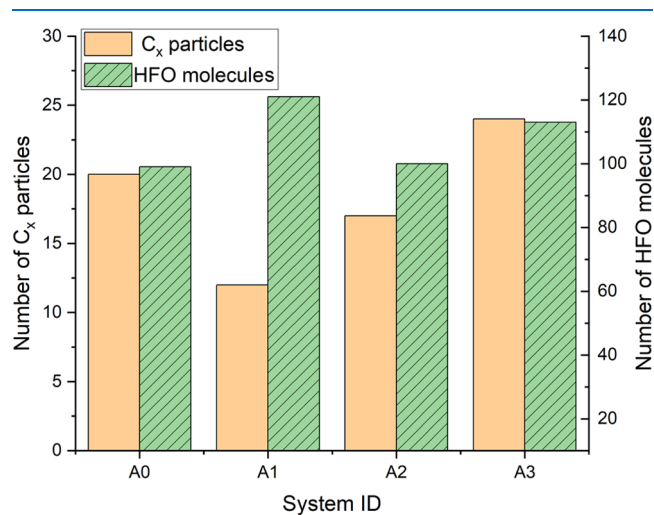


Figure 1. ReaxFF simulation results for the HFO mixture with different buffer gases.

It can be seen from Figure 1 that the number of C_x particles generated in the A1 and A2 systems is less than that in the A0 system, while the A3 system generates the most C_x particles. On the other hand, the decomposition ratio of HFO in the A1 and A3 systems is lower than that in the A0 system. Meanwhile, the decomposition degree of HFO in the A2 system is basically the same as that in the A0 system. However, the amount of C_x particles generated in the system is directly related to the amount of solid precipitation,²³ and the degree of HFO decomposition, at the same time, is also closely related to the gas insulation performance. After comprehensively considering these two factors, it can be considered that the A1 system (HFO–N₂–O₂ gas mixture) has a better solid precipitate suppression effect and application potential.

In addition to the three candidate buffer gases (O_2 , CO_2 , CF_4) considered in this study, there are many other potential buffer gases that may achieve the goal of suppressing the HFO solid products. Therefore, a detailed analysis of the reasons for obtaining the above simulation results will help to understand the microscopic decomposition mechanism of the HFO gas mixture system under the action of different buffer gases, which can provide more helpful information for the screening of other possible buffer gases that could inhibit the precipitation of HFO solid products.

2.1.2. Influence Mechanism of Buffer Gases on the HFO Solid Decomposition Products. As mentioned above, reducing the decomposition of HFO and accelerating the consumption of C_x particles are the main ideas for suppressing the solid decomposition products of HFO. To analyze the impact mechanism of the buffer gas on the degree of decomposition of HFO, we first obtained the main decomposition path of HFO by tracking the motion trajectory of molecules (atoms) in the simulation process, as shown in Table 1.

Table 1. Typical Decomposition Paths of HFO and its Reaction Rate Constants^a

ID	reaction path	reaction rate constant
(1)	$C_3H_2F_4 \rightarrow C_3HF_4 + H$	6.51×10^{-8}
(2)	$C_3H_2F_4 \rightarrow C_3H_2F_3 + F$	3.91×10^{-8}
(3)	$C_3H_2F_4 \rightarrow CF_3 + H + C_2HF$	2.58×10^{-8}
(4)	$C_3H_2F_4 + H \rightarrow C_3H_3F_4$	1.22×10^{-9}
(5)	$C_3H_2F_4 + F \rightarrow C_3H_2F_5$	7.78×10^{-10}

^aNote: the molecular formula of HFO1234Ze(E) is $C_3H_2F_4$.

The reaction paths (1), (2), and (3) given in Table 1 are all simple bond-breaking reactions, so their reaction rates mainly depend on the physicochemical properties of the HFO molecule itself and the external factors such as temperature. These reaction paths will play a leading role in the initial

decomposition of HFO. As the reaction progresses, the concentrations of H, F, and CF_3 radicals in the system will affect the reverse reaction rates of the reaction paths (1), (2), and (3) to a certain extent. For reaction paths (4) and (5), the reaction rates are mainly affected by the H atoms and F atoms generated by the decomposition of HFO in the system. Comparing the reaction rate constants in Table 1, it can be found that free H atoms have a greater influence on the decomposition of HFO than free F atoms in the subsequent reaction process.

Next, we will further analyze the influence mechanism of different buffer gases on the amount of HFO solid precipitates based on the product curves of different buffer gas reaction systems. The change curves of reactants and main decomposition products of the A0–A3 system are shown in Figure 2. The comparison of product contents in different systems is shown in Figure 3. The typical reaction paths related to the following analysis are shown in Table 2.

Comparing Figure 2a,b, it can be seen that after a small amount of O_2 is introduced into the HFO– N_2 mixture, the free O atoms formed by the decomposition of O_2 are easily combined with the free H atoms generated by the decomposition of HFO. During the 1000 ps simulation, the average number of H atoms in the A1 system was 88, which was 8% lower than that of the A0 system (96). Therefore, the presence of O_2 inhibits the number of free H atoms in the system to a certain extent, thereby reducing the decomposition of HFO through the reaction path (4). Less decomposition of HFO molecules can inhibit the generation of C_x particles from the source because the C-containing groups generated by the decomposition of HFO will be further decomposed under the influence of high temperature or other groups (such as reaction paths (6)–(10)) to generate C_x particles. On the other hand, stable molecules such as CO, CO_2 , and COF_2 are generated (reaction paths (11)–(14)) in the A1 system, which consumes the C_x particles directly or indirectly. Under the joint action of the above two factors, the A1 system exhibits an excellent

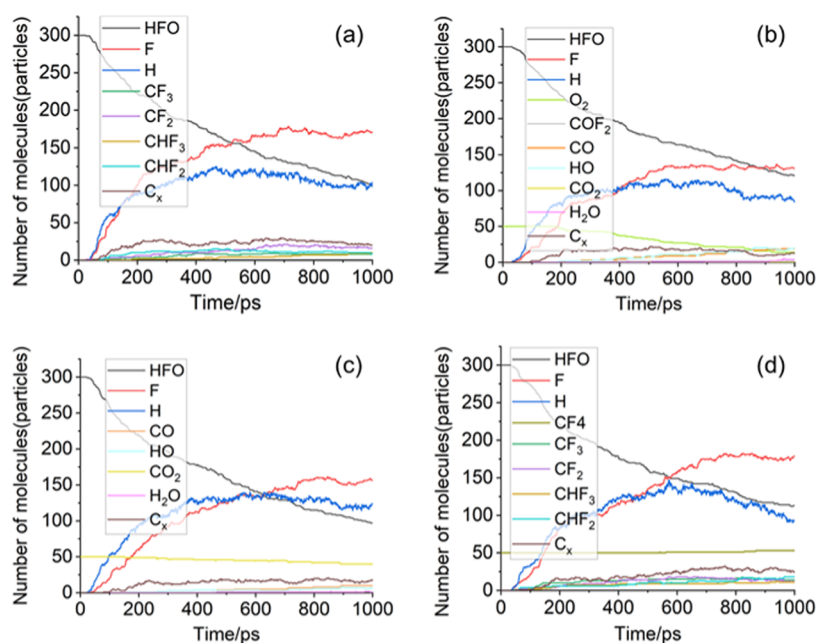


Figure 2. Change curves of reactants and the main decomposition products in the (a) A0 system, (b) A1 system, (c) A2 system, and (d) A3 system.

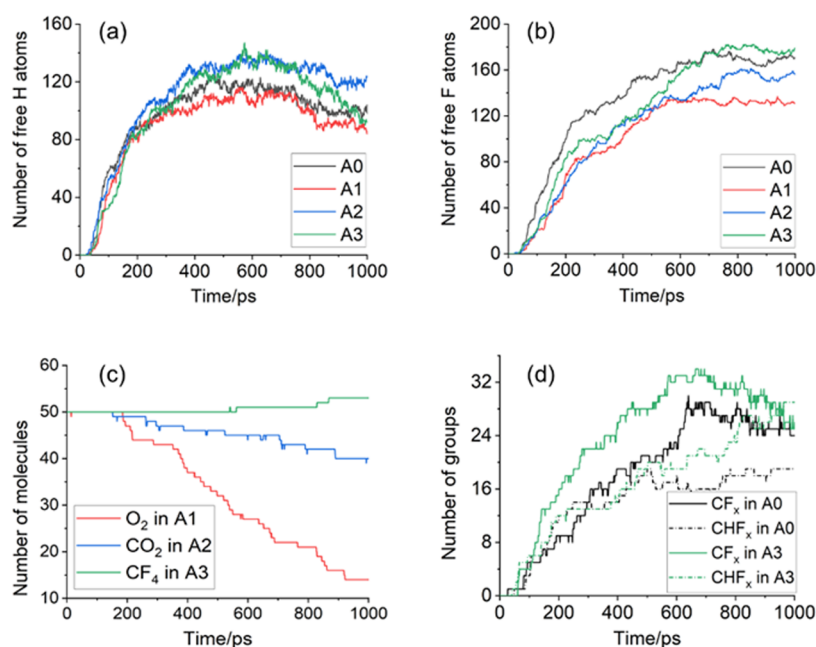


Figure 3. Comparison of main molecules (groups) contents in different systems with a number of (a) free H atoms; (b) free F atoms; (c) O₂, CO₂, and CF₄ molecules; and (d) CF_x and CHF_x groups.

Table 2. Typical Reaction Paths Related to the Formation and Consumption of C_x Particles and the Formation of Other Key Products

ID	reaction path	ID	reaction path
(6)	C ₃ F → C ₃ + F	(12)	O + C ₂ → CO + C
(7)	C ₃ F + N → C ₂ + CNF	(13)	C + O ₂ → CO ₂
(8)	C ₂ HF → C ₂ + HF	(14)	CF ₃ + O → COF ₂ + F
(9)	C ₂ F → C ₂ + F	(15)	C ₂ H + CF ₃ → CHF ₃ + C ₂
(10)	C ₃ → C ₂ + C	(16)	C ₂ HF + CF ₂ → CHF ₂ + C ₂ F
(11)	O ₂ + C ₃ → C ₂ + CO ₂		

suppression effect of HFO solid precipitates. At the same time, less HFO decomposition can also improve the stability of the HFO gas mixture insulation performance to a certain extent.

It can be seen from Figure 3c that, as a stable oxidation product, the buffer gas CO₂ has a lower reaction activity than O₂ and so its decomposition amount during the reaction is less than O₂. In addition, because a CO₂ molecule can only provide one O atom (in this case, no new C particles are generated) for consuming C_x particles or H atoms in the system, the inhibitory effect of CO₂ on the decomposition amount of HFO and the promotion effect of CO₂ on the consumption of C_x particles are not as obvious as that of O₂.

From Figure 3d, it can be found that the presence of CF₄ promotes the generation of CF_x groups in the A3 system. The average content of CF_x groups during the 1000 ps simulation increases by 30% compared to the A0 system. According to Table 1, the increase of the concentration of CF₃ groups will promote the reverse reaction rate of the reaction path (3), which will reduce the amount of HFO decomposition. In addition, the average content of CHF_x in 1000 ps is 21% higher than that of the A0 system. This is because the CF_x particles present in the A3 system are more likely to take away the H or F atoms from the unstable C_xH_y or C_xF_y groups to form CHF₂, CHF₃, and C_x particles (reaction paths (15)–(16)). Therefore, although the CF₄ buffer gas suppresses the decomposition of HFO, it increases the generation of C_x

particles to a considerable degree. In short, the gas mixing scheme of the A3 system did not achieve the expected research purpose of suppressing the precipitation of solid products.

From the above analysis, it can be inferred that inhibiting the decomposition of HFO and promoting the consumption of C_x particles all have a considerable impact on inhibiting the formation of the HFO solid precipitates. Therefore, in an ideal situation, the buffer gas needs to meet the two requirements at the same time to achieve the best suppression effect of the solid products. Among the several candidate buffer gases studied in this paper, only O₂ satisfies these two requirements well and stands out in the screening process. In the following section, we will consider O₂ as a potential buffer gas, and carry out further simulation and experimental research on the decomposition and insulation properties of the HFO–N₂–O₂ gas mixture.

2.2. Study on the Decomposition Characteristics of the HFO–N₂–O₂ Gas Mixture. **2.2.1. Influence of O₂ Content on the Decomposition Characteristics of the HFO Gas Mixture.** After performing 1000 ps simulation according to the settings of Section 4.1, the number of C_x particles (average value during 900–1000 ps) and the number of remaining HFO molecules in systems with different O₂ contents are shown in Figure 4. Figure 5 shows the change curves of the reactants and the main decomposition products in the simulation systems with different O₂ contents.

It can be seen from Figure 4 that with the increase of the O₂ content, the number of C_x particles generated by the decomposition of HFO changes in a “V” shape. The O₂ content in the B1 system is very small and so its inhibitory effect on HFO solid products is not obvious. When the O₂ content reached 3.33% (B2 system), the amount of C_x decreased significantly compared with that of the A0 system and the decrease rate reached 48%. Furthermore, as the content of O₂ increases, the amount of C_x gradually increased. Compared with the A0 system, the number of C_x in the B4 system increased by 13%. On the other hand, under the

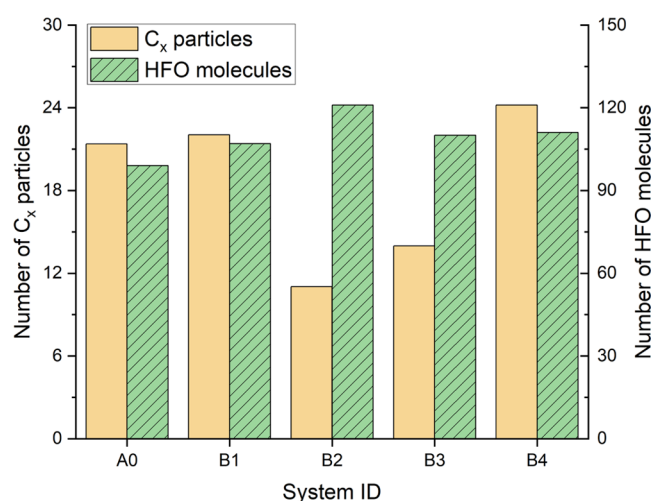


Figure 4. Number of C_x particles and HFO molecules in the simulation system.

influence of O₂, the decomposition ratio of HFO in each system decreased to varying degrees. Compared with the decomposition ratio of HFO in the A0 system (67%), the decomposition ratio of HFO in the B2 system (60%) decreased significantly. However, the decomposition rate of HFO in B3 and B4 systems slightly increases than that of B2, reaching about 63%. The reason for this result can be explained from the perspective of the amount of O₂ involved in the reaction. It can be seen from Figure 5b that in the system with higher O₂ content, more free O atoms are generated. The analysis in Section 2.1 points out that free O atoms can reduce the probability of HFO decomposition via reaction path (4) by capturing free H atoms and can reduce the C_x content by generating CO and CO₂ products. However, when the content of free O atoms increases to a certain extent, the probability of O atoms directly attacking HFO molecules or C_xH_y and C_xF_y groups increases, thereby weakening the effect of O₂ in inhibiting the HFO decomposition and C_x particle generation. The related typical reaction paths are shown in Table 3.

According to the above analysis, the oxygen content in the HFO–N₂–O₂ mixture should be controlled at an appropriate level. The B2 system shows the best inhibition effects of solid products and the HFO decomposition.

In addition to the solid decomposition products, the presence of O₂ will also affect the generation mechanism of other gas decomposition products such as CF₄ and CHF₃, which may have an important impact on the long-term insulation performance of the system.²² Therefore, it is necessary to analyze the decomposition characteristics of the HFO mixture under the influence of different O₂ contents.

It can be seen from Figure 5c that with the increase of the O₂ content in the system, the number of CO molecules produced by the reaction increases at first and then decreases. The B2 system produces the most CO molecules. The H₂ content produced by the reaction is generally opposite to the change trend of the O₂ content. The content of H₂ generated in the B4 system is 36% lower than that of the A0 system. Trace amounts of H₂O molecules are generated in simulation systems with different O₂ contents but the O₂ content has no obvious influence on the amount of H₂O molecules generated. It can be seen from Figure 5g,h that the number of CF_x and CHF_x groups generated by decomposition in the B2 system is

the smallest, which to a certain extent reflects that the B2 system has better long-term insulation properties.

2.2.2. Influence of Temperature and Pressure on the Decomposition Characteristics of the HFO Gas Mixture. The number of C_x particles generated at different reaction temperatures and different gas pressure (average value during 900–1000 ps) is shown in Figure 6. The change curves of the reactants and main decomposition products in the simulation systems at different reaction temperatures and gas pressures are shown in Figures S1 and S2 (tables and figures whose label starts with “S” can be found in the Supporting Information).

First, we will analyze the effect of temperature on the decomposition characteristics of the HFO–N₂–O₂ gas mixture. It can be seen from Figure 6a that as the temperature increases, the number of C_x particles generated in the system first decreases and then increases. At 1200 K, the number of C_x particles generated by HFO decomposition is controlled at the lowest level. It can be seen from Figure S1a that the number of HFO molecules decomposed at 800 K is relatively small; however, the number of C_x particles produced at this temperature is more than that at 1200 K. This is mainly because at 800 K, the number of free O atoms in the system is relatively small and the particle migration rate is relatively low. The combination of these two factors reduces the probability of O atoms encountering C_x particles. Even if the encounter occurs, the probability that the particles have sufficient energy to overcome the reaction barrier and produce oxygen-containing products is small. As a result, the C_x particles produced by the decomposition of HFO cannot be effectively consumed. At higher reaction temperatures, the proportion of HFO gas decomposition increases significantly. However, due to the relatively low proportion of O₂ in the gas mixture, the difference between the C_x generated by HFO decomposition and C_x particles consumed by O atoms reaches the minimum at 1200 K. When the temperature continues to increase, even if O₂ fully participates in the reaction, a lot of C_x particles are still accumulated in the system. Therefore, it is speculated that higher discharge energy will lead to more solid precipitation. That is, the severity of the discharge fault is closely related to the amount of solid precipitation.

It can be seen from Figure S1 that the decomposition rate of HFO is greatly affected by the temperature. At higher temperatures, the decomposition amount of HFO is greater, which to a certain extent means that more solid products could be generated. At 800 and 1200 K, the HFO content curve basically shows a linear downward trend. However, when the temperature reaches above 1600 K, the HFO decomposition curve shows a clear logarithmic shape, that is, it decomposes rapidly at first and then the decomposition rate gradually decreases. Since the discharge intensity is directly related to temperature, optimizing the electrode structure or treating the electrode to reduce the discharge intensity is one of the possible methods to reduce the precipitation of HFO solid products.

On the other hand, O₂ molecules start to decompose after 300 ps simulation at 800 K. This is mainly because the direct decomposition of the O=O double bond requires a large amount of energy to be absorbed. However, under the action of the free H and F atoms generated by the decomposition of HFO, the reaction barrier that needs to be overcome to break the O=O double bonds in O₂ is greatly reduced. Therefore, when the H and F atoms in the system accumulate to a certain

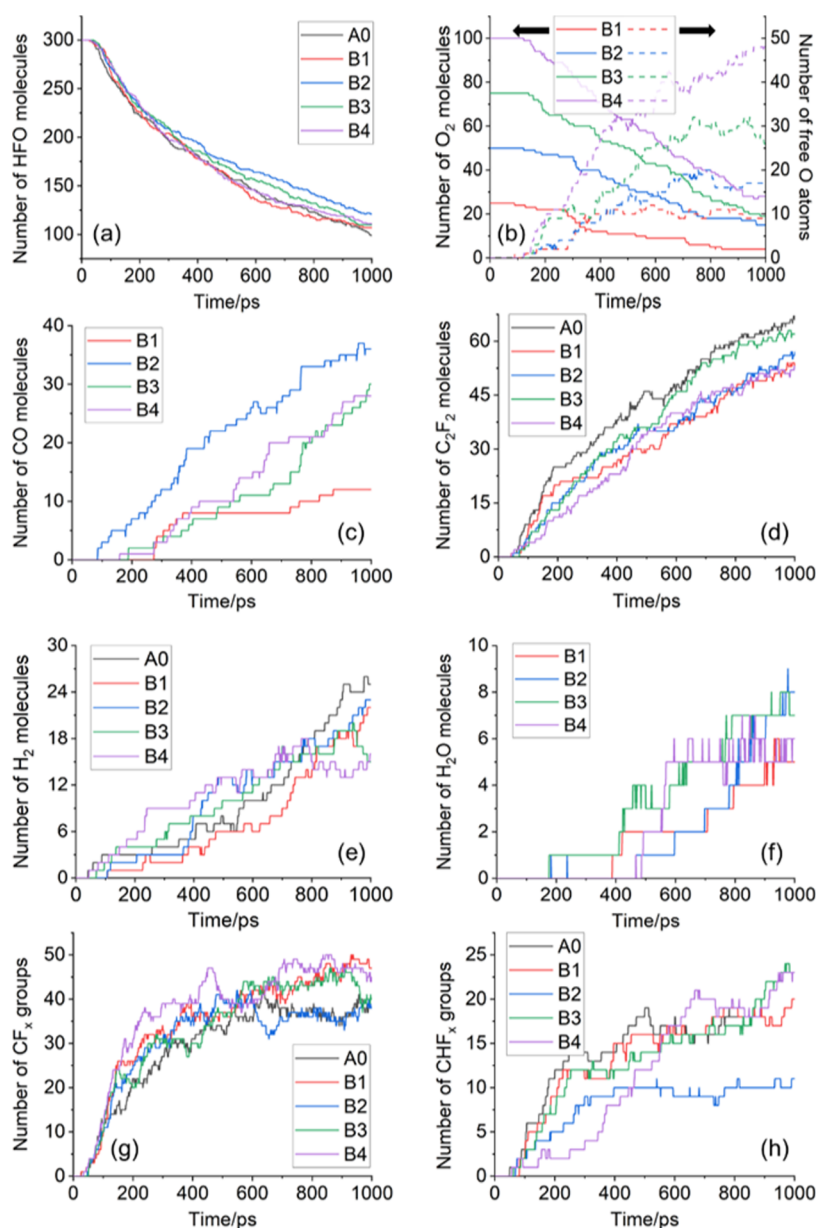


Figure 5. Change curves of the reactants and main decomposition products in the simulation systems with different oxygen contents: (a) a number of HFO molecules; (b) a number of O₂ molecules; (c) a number of CO molecules; (d) a number of C₂F₂ molecules; (e) a number of H₂ molecules; (f) a number of H₂O molecules; (g) a number of CF_x groups; and (h) a number of CHF_x groups.

Table 3. Typical Reaction Paths of O Atoms Directly Attacking HFO, C_xF_y, and C_xH_y

ID	reaction path
(17)	$O + C_3H_2F_4 \rightarrow CF_3 + C_2HFO + H$
(18)	$O + C_3F \rightarrow C_2 + COF$
(19)	$O + C_2H \rightarrow C_2 + OH$

extent, the decomposition of O₂ atoms can be effectively promoted.

At the reaction temperature of 800 K, no H₂O molecules were generated in the system. At temperatures ranging from 1200 to 2000 K, the content of H₂O generated in the system is basically at the same level. Compared with the content of other gas products, the amount of H₂O generated is very small. So, the higher fault temperature will not have a significant impact on the moisture content of the HFO–N₂–O₂ gas mixture after

a breakdown. The contents of C₂F₂, H₂, CF_x, and CHF_x molecules (groups) increase significantly with the increase of the reaction temperature. The contents of C₂F₂ and H₂ molecules showed a certain saturation tendency at the end of the 1000 ps simulation but still maintained a certain increasing rate. The contents of CF_x and CHF_x groups had reached saturation at about 400 ps. The contents of CF₄ and CHF₃ can be used to characterize the severity of discharge failures in the HFO–N₂–O₂ gas mixture insulation equipment.

Next, the influence of pressure on the decomposition characteristics of the HFO–N₂–O₂ gas mixture will be analyzed. It can be seen from Figure 6b that as the gas pressure increases, the number of C_x particles produced by the reaction at the same temperature shows a decreasing trend. This is mainly because the higher gas pressure could increase the number of free H atoms, F atoms, and O atoms in the unit space, thus promoting the combination process of these

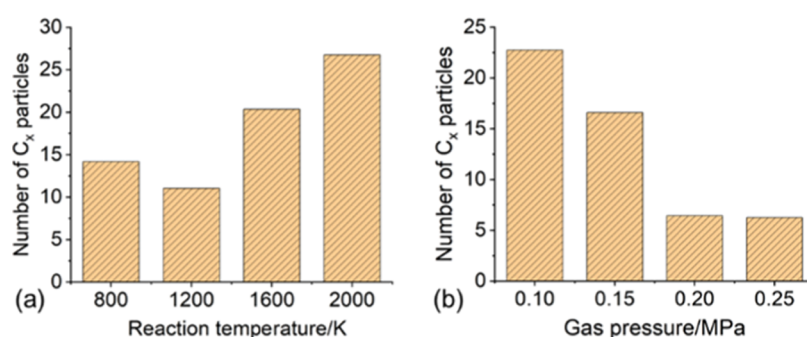


Figure 6. Number of C_x particles generated by the decomposition of the HFO–N₂–O₂ gas mixture at different (a) reaction temperatures and (b) gas pressures.

particles with C_x particles. The number of C_x particles generated under 0.20 MPa pressure is only about one-fourth of that under 0.10 MPa. However, continuing to increase the pressure of the system has little effect on the suppression of the number of C_x particles. This is because the increase in pressure will also increase the probability of H, F, and O attacking HFO molecules, thus promoting the decomposition of HFO. It can be seen from Figure S2a that compared with 0.20 MPa, the HFO decomposition amount at 0.25 MPa increased from 73 to 78%. More HFO decomposition will yield more C_x particles. Under the influence of these two competitive factors, the number of C_x particles approaches the minimum value at 0.20 MPa. The simulation results revealed that appropriately increasing the pressure of the HFO–N₂–O₂ gas mixture is a possible way to suppress the formation of solid products.

It can be seen from Figure S2 that the decomposition ratio of HFO and O₂ increases slightly with the increase of gas pressure. Under different pressures, the decomposition rate of HFO in the initial stage is basically the same. It was not until about 50 ps that the curves showed relatively obvious differences. The analysis in the article shows that HFO is more likely to decompose when combined with free radicals such as H or F. Therefore, the increase in pressure mainly affects the decomposition rate of HFO by increasing the probability of HFO being attacked by other free radicals.

The formation of CO molecules is greatly affected by the gas pressure. The amount of CO molecules generated at 0.15 MPa is 50% higher than that at 0.10 MPa. However, when the gas pressure continues to increase, the amount of CO generated decreases on the basis of the amount at 0.15 MPa. Increasing the pressure of the gas mixture will significantly increase the content of H₂O generated by decomposition. When the gas pressure reaches 0.25 MPa, the amount of H₂O generated in the reaction system is about two times that under 0.10 MPa. Therefore, when considering the suppression of the solid product precipitation by increasing the gas pressure, additional attention needs to be paid to the influence of the generated H₂O on the insulation strength of the gas–solid insulation system. When the system pressure is increased from 0.10 to 0.15 MPa, the contents of H₂ and C₂F₂ will increase slightly; however, in the pressure range of 0.15–0.25 MPa, the pressure has little effect on the production of H₂ and C₂F₂ molecules. The content of CF_x groups is not significantly affected by air pressure. The content of CHF_x groups increases as the pressure of the gas mixture increases and reaches saturation at 0.20 MPa.

2.2.3. Formation Mechanism of the Main Products During the Diffusion Cooling Process. In this study, ReaxFF

MD simulation was used to simulate the decomposition process of HFO gas molecules at high temperatures caused by the discharge fault. After 1000 ps ReaxFF MD simulation, in addition to stable products such as C₂F₂, CO, and H₂, there are also many intermediate transition products such as H, F, CN, CF₂, and CF₃ with higher reactivity in the simulation system. The content of the main decomposition products in the simulation system at different reaction temperatures can be found in Figure S3. In the actual gas chamber, these intermediate products will diffuse into the lower temperature space around the discharge area and form various stable decomposition products through a relatively slow free radical recombination process.

Based on the stable products and free radicals obtained from MD simulations, the energy changes of various possible reaction paths are obtained by density functional theory (DFT) calculations. In the calculation, the Gaussian 09 quantum chemistry package and M062X/6-311+G(d,p) level were used.²⁴ The calculated reaction paths and relative energy changes are shown in Table 4.

Table 4. Possible Reaction Paths and Relative Energy Changes (M06-2X/6-311+G(d,p))

ID	reaction path	standard reaction enthalpy (kJ/mol)
P1	CF ₃ + CF ₃ = C ₂ F ₆	−405.48
P2	CF ₂ + CF ₂ = C ₂ F ₄	−302.03
P3	CF ₃ + F = CF ₄	−532.47
P4	C ₂ F ₂ + 2F = C ₂ F ₄	−814.96
P5	C ₂ F ₄ + 2F = C ₂ F ₆	−810.97
P6	CF ₃ + CCF = CF ₃ CCF	−531.04
P7	CF ₃ + CN = CF ₃ CN	−480.48
P8	CO + O = CO ₂	−775.16
P9	H + OH = H ₂ O	−485.76
P10	CF ₃ + H = CHF ₃	−442.44
P11	C ₂ F ₂ + 2H = C ₂ F ₂ H ₂	−734.73

It can be seen from Table 4 that the reaction paths P1–P11 are all exothermic reactions. For this type of reaction, the more negative the standard reaction enthalpy, the greater the heat released by the reaction and, to a certain extent, the easier the reaction occurs.

Combining Figure S3 and Table 4, it can be seen that at the end of the 1000 ps reaction, the content of C₂F₂ and F accumulated in the system is large and so it is easy to generate C₂F₄ through path P4. On this basis, C₂F₄ can further generate C₂F₆ through path P5. At the same time, C₂F₂ can also combine with H atoms through path P12 to generate C₂F₂H₂.

The CO accumulated in the system can further react with free O atoms through path P9 to generate CO₂. Taking into full consideration of the free radical content in the system and the energy change of the reaction path, it can be inferred that C₂F₄, C₂F₆, CO₂, C₂F₂H₂, CF₃CCH, and CF₃CCF are the main products generated in the diffusion cooling process. This result is basically consistent with the HFO decomposition products obtained by gas chromatography in the previous work of our research team.²² However, it does not reflect the formation of *cis*-C₃H₂F₄ (the isomer of HFO1234Ze(E)), C₂HF₃, and CF₃CHCF₂.

2.3. DC Breakdown and the Solid Product Precipitation Characteristics of the HFO–N₂–O₂ Ternary Gas Mixture.

2.3.1. Solid Product Precipitation Characteristics. Using the experimental settings in Section 4.2, experiments on the breakdown characteristics of HFO–N₂–O₂ ternary gas mixtures under different pressures were carried out. Table 5

Table 5. Mass of Solid Decomposition Products on the Plate Electrode (mg)

	after 10 consecutive breakdowns		after 20 consecutive breakdowns	
	0.10 MPa	0.15 MPa	0.20 MPa	0.25 MPa
HFO–N ₂	1.1	0.8	0.9	0.8
HFO–N ₂ –O ₂	0.4	0.4	0.3	0.4

shows the mass measurement results of the solid decomposition products on the plate electrode before and after the breakdown test. The surface state of the ball electrode after the breakdown experiment is shown in Figure S4.

It was found that the diameter of the area covered by the black solid products on the ball-plate electrode was about 1.38 cm. Most of the black products on the electrode surface can be easily removed. However, the black product within a diameter of about 3 mm (the area where the breakdown channel occurs) near the minimum distance of the ball-plate electrode is tightly attached and cannot be directly removed, as shown in Figure S4b. This is because a large amount of energy is released when the gas gap breakdown occurs. The high temperature near the breakdown channel causes the black product to adhere tightly to the surface of the ball electrode. In addition, after a single breakdown test of the HFO–N₂–O₂ gas mixture, a large area of black solid precipitation was also observed. Combining the experimental phenomena with the electric field simulation results, it can be found that the area where the black solids are distributed is basically the same as the area where the electric field is severely distorted.

Based on the above analysis, it is speculated that the black solid decomposition products are mainly generated by the corona discharge between the ball plate electrodes before the air gap breakdown. However, the reliability of this speculation still cannot be fully proved according to the current experimental results and so further research is needed.

Furthermore, the area of the solid decomposition product adhesion area on the electrode surface in HFO–N₂ and HFO–N₂–O₂ environments under the same pressure was compared. The results show that the diameter of the black solid distribution area did not change significantly, but the color near the edge of the black area was slightly lighter after adding O₂. It can be seen from Table 5 that under the same pressure, the mass of solids decomposed in the HFO–N₂–O₂ gas mixture is significantly reduced compared with that in the

HFO–N₂ gas mixture. In addition, with the increase of gas pressure, the solid content generated under the same gas shows a downward trend. The above two experimental phenomena are consistent with those observed in ReaxFF MD simulation.

2.3.2. DC Breakdown Characteristics. To visually compare the effect of O₂ on the breakdown voltage of the gas mixture, we calculated the average value and the mean square error of the 2nd–6th breakdown voltage under each experimental setting (the reason for ignoring the first breakdown voltage will be explained later); the result is shown in Figure 7. It can be

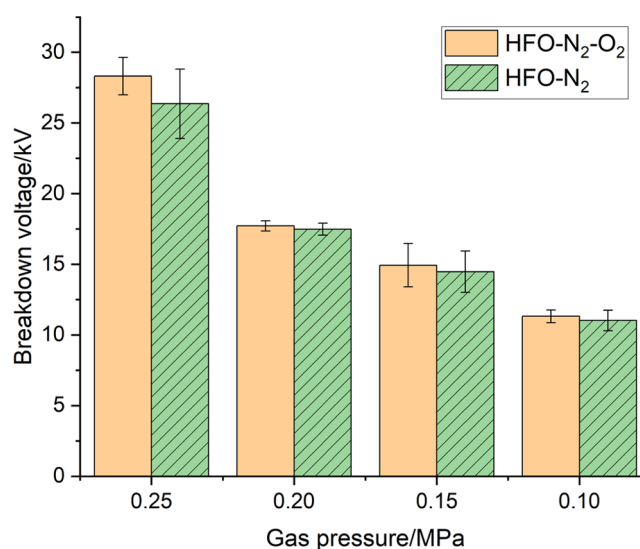


Figure 7. Breakdown voltage of the HFO–N₂–O₂ gas mixture at different gas pressures.

seen from Figure 7 that after adding O₂ to the HFO–N₂ gas mixture, the breakdown voltage at the same pressure increases slightly. This is because the electronegativity of oxygen is stronger than that of nitrogen and so O₂ is better than N₂ in absorbing free electrons, which makes collision ionization relatively weaker during discharge.

The self-recovery characteristics and breakdown voltage dispersion degree of the HFO gas mixture are important indicators for evaluating gas insulation performance. The change of breakdown voltage with the number of breakdowns is shown in Figure 8. Comparing the breakdown voltage of HFO–N₂ and HFO–N₂–O₂ gas mixtures at the same pressure, it can be found that the addition of O₂ slows down the drop rate of the breakdown voltage to a certain extent. At 0.25 MPa pressure, for example, the fitting curve slope of the HFO–N₂–O₂ gas breakdown voltage is –0.2685, which is 45% lower than that of the HFO–N₂ gas mixture (–0.4887). In addition, the presence of O₂ also reduces the dispersion degree of breakdown voltage, and this phenomenon is more obvious under relatively high gas pressure.

In addition, it can be observed from Figure 8 that regardless of the presence or absence of O₂, there is a relatively large voltage drop (in some cases, the drop can reach 15–20%) between the first breakdown voltage and the second breakdown voltage of the HFO mixture. After the second breakdown, although the subsequent breakdown voltage will gradually decrease with the increase in the number of breakdowns, the decrease is far less than the drop between the first and second breakdown voltages. Based on experimental phenomena, it is speculated that the black

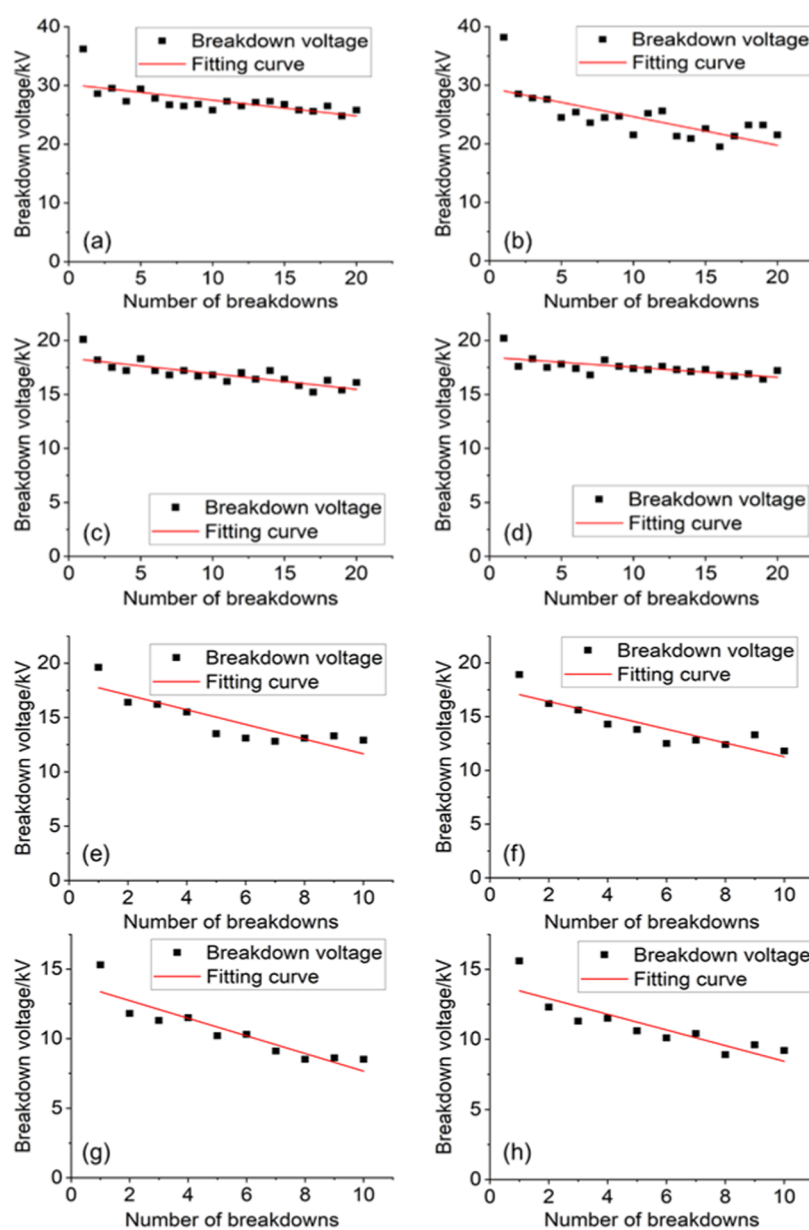


Figure 8. Variation of the breakdown voltage with breakdown times: (a) 0.25 MPa HFO-N₂-O₂; (b) 0.25 MPa HFO-N₂; (c) 0.20 MPa HFO-N₂-O₂; (d) 0.20 MPa HFO-N₂; (e) 0.15 MPa HFO-N₂-O₂; (f) 0.15 MPa HFO-N₂; (g) 0.10 MPa HFO-N₂-O₂; and (h) 0.10 MPa HFO-N₂.

decomposition products attached to the electrode are the main reason for the initial voltage drop. When solid products are attached to the electrode surface, the surface roughness increases significantly and there are many protrusions on the microstructure. Therefore, the electric field on the electrode surface will be greatly distorted, which in turn is more likely to cause partial discharge and even breakdown.

It is noticed that the addition of O₂ has almost no obvious effect on the initial voltage drop. This may be because the electrode surface is in good condition before the first breakdown and so the corona discharge intensity is relatively low, and the corresponding reaction zone temperature is also lower. At this time, O₂ cannot fully participate in the reaction to consume C_x particles (this phenomenon is consistent with the simulation result of the lower reaction temperature). In the subsequent breakdown process, however, the solid precipitates caused more serious corona discharge; at this time, O₂

inhibition of the solid precipitate was more obvious. This can explain why O₂ improves the degree of subsequent breakdown voltage drop.

Based on the above analysis, it can be concluded that adding a small amount of O₂ to the HFO-N₂ gas mixture can effectively inhibit the generation of solid decomposition products and will not negatively affect the gas insulation characteristics. Therefore, O₂ is a promising buffer gas for suppressing HFO solid products, and it is worth continuing to conduct more in-depth research.

2.4. Discussion. 2.4.1. Universality of Research Methods.

The discussion in the previous section shows that the ReaxFF MD simulation and experimental results have satisfactory consistency in the characterization of solid decomposition products and the selection of HFO gas mixing schemes. However, the novel analysis method proposed in this paper is not limited to HFO. With the support of a reliable ReaxFF

force field, the application of ReaxFF MD simulation has great expansibility.

The ReaxFF force field used in this study comes from the literature research, mainly including C, H, F, O, and N elements and has been widely used in the study of the decomposition characteristics of gases containing these elements. The above analysis can further illustrate that the gas mixing scheme screening method based on the ReaxFF MD simulation proposed in this paper can also provide effective technical support for solving the problem of solid precipitation suppression of other environmentally friendly insulating gas in the C/F/O/N system (such as C_4F_7N , $C_5F_{10}O$, etc.).

2.4.2. Problems that Require Further Study. In the decomposition experiment of the insulating gas mixture $C_4F_7N-N_2-O_2$, which has similar properties to the HFO- N_2-O_2 gas mixture, the COF_2 molecule is detected. Relevant studies have shown that COF_2 has strong biological toxicity and is highly corrosive.²⁵ Therefore, the production of this substance will cause damage to the health of operation and maintenance personnel and the safe operation of equipment. Under the simulation setting of this article (3.33% oxygen content), a few COF_2 molecules are generated at 800–2000 K. However, considering that the temperature of the fault discharge area in the gas-insulated equipment may be much higher than the temperature used in the simulation, it is necessary to carry out further experimental research on the content of harmful substances such as COF_2 in the HFO- N_2-O_2 gas mixture discharge decomposition products.

According to the experimental research carried out in this article, it is found that although the addition of O_2 to HFO- N_2 can inhibit the formation of solid products to a large extent, the problem of initial pressure drop remains unresolved. The decrease of the gas insulation strength after the initial breakdown is a huge test for equipment insulation so further research is urgently needed. On the other hand, to prove that O_2 will not negatively affect the insulation properties of the HFO gas mixture, in this paper, we carried out an experimental study on the air gap breakdown characteristics in the slightly uneven electric field under a negative DC voltage. However, to fully demonstrate the application potential of O_2 as a buffer gas for suppressing the solid products, further research is needed under different voltage conditions (such as AC voltage, impulse voltage, and AC/DC superimposed impulse voltage) and different electric field uniformities.

3. CONCLUSIONS

In this paper, simulations and experiments are performed to study the inhibitory effect of the buffer gas on the HFO solid decomposition products. The main conclusions obtained from this study are as follows:

- (1) The inhibitory effect of O_2 on the formation of HFO solid precipitates is better than that of CO_2 and CF_4 . With the increase of the O_2 content in the HFO- N_2-O_2 gas mixture, the content of solid precipitates first decreases and then increases and reaches the minimum when O_2 accounts for 3.33% of the gas mixture, in which case the precipitate content decreased by 48% compared with that in the HFO- N_2 gas mixture. In addition, the content of solid precipitates is proportional to the reaction temperature and inversely proportional to the gas pressure.

- (2) Experimental research shows that compared with HFO- N_2 (20/80%), the DC breakdown voltage of the HFO- N_2-O_2 (20/76.67/3.33%) gas mixture increases slightly and the breakdown voltage dispersion degree is reduced. In addition, the continuous breakdown voltage drop rate of HFO- N_2-O_2 is also reduced to a certain extent. After the same number of breakdown tests, the mass of the solid products attached to the electrode is significantly reduced under the influence of O_2 and the reduction percentage could reach more than 50%. Therefore, O_2 as a buffer gas has a prominent application prospect in achieving the suppression of HFO solid precipitates.
- (3) A buffer gas screening method for the suppression of the HFO solid decomposition products based on ReaxFF MD simulation is proposed. The cross-validation of simulation and experimental results supports the validity of the proposed research method. Based on the expandability of ReaxFF simulation, this method can be applied to solve the similar problem of environmentally friendly insulating gases in the C/F/O/N system such as C_4F_7N and $C_5F_{10}O$.

4. METHODS

4.1. Simulation Methods. The ReaxFF force field used in this study contains C, H, O, N, and F elements,²⁶ and has been applied to the study of the pyrolysis characteristics of HFO gas.¹³ To avoid the drastic change of system energy in the initial stage of simulation, the molecular structures of HFO, N_2 , and candidate buffer gases were optimized under the selected force field. Then the builder module integrated into AMS software is used to establish the periodic simulation model. The total number of molecules and gas pressure in the simulation system is set to 1500 and 0.1 MPa, respectively. Given the number of gas molecules, the gas pressure and temperature (298 K), the side length of the simulation cubic box should be 395.21 Å according to the ideal gas law. Based on the research results on the HFO gas insulation characteristics in the literature,^{13,27} the HFO- N_2 (20/80%) gas mixture system with prominent application potential is selected as the benchmark in this research, identifying as A0. On this basis, keeping the content of HFO unchanged and then replacing 50 N_2 molecules with O_2 , CO_2 , or CF_4 molecules, respectively, to form three HFO ternary gas mixture systems, identifying as A1–A3. The detailed parameters of each simulation system are shown in Table S1.

The MD simulations in this study are all carried out under canonical ensemble (NVT). The temperature control method is Berendsen, the damping constant is 100 fs, and the simulation time step is 0.25 fs. First, 10 ps MD simulation is performed at a temperature of 298 K to make the system reach an equilibrium state. Then, the temperature of the simulation system is increased at a rate of 0.1 K/fs to 1200 K,¹³ and this temperature is maintained until the end of the simulation. A total of 1000 ps simulation was performed.

Using the same modeling method as before, 25, 50, 75, and 100 N_2 molecules were replaced with O_2 molecules, respectively, to establish four simulation systems with different oxygen contents, denoted B1–B4. The parameters of the simulation systems are shown in Table S2. Based on the gas mixing ratio of the B2 system model, four simulation models with 0.10, 0.15, 0.20, and 0.25 MPa gas pressures were

established, denoted C1–C4. The parameter settings of the simulation system are shown in Table S3.

For the simulation systems in Tables S2 and S3, after performing 10 ps NVT relaxation at 298 K, the temperature of the simulation system is increased to 1200 K at a rate of 0.1 K/fs and maintained until the end of the 1000 ps simulation. To explore the effect of reaction temperatures on the decomposition characteristics of the HFO–N₂–O₂ gas mixture, a series of ReaxFF MD simulations were carried out in the B2 system model. After 10 ps NVT relaxation at 298 K, the temperatures of the simulation system were increased to 800, 1200, 1600, and 2000 K, respectively, at a rate of 0.1 K/fs and kept until the end of the 1000 ps simulation.

4.2. Experimental Methods. In this study, the DC voltage is provided by the HYAC/DC-300 AC/DC power source. The breakdown test for the HFO–N₂–O₂ gas mixture is carried out in the gas insulation performance test platform as shown in Figure 9a. The radius of the ball electrode used in the

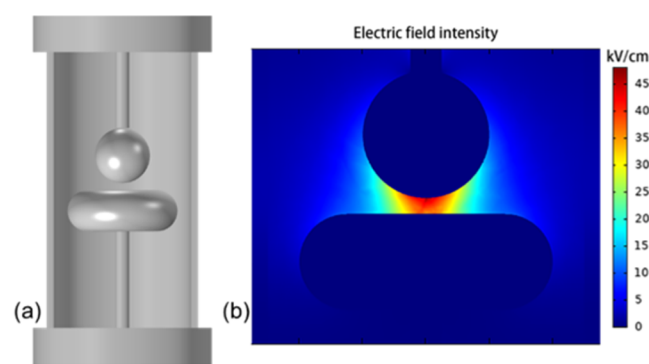


Figure 9. Related information of the gas insulation performance test platform: (a) structural diagram and (b) electric field simulation results.

experiment is 40 mm and the distance between electrodes is 5 mm. COMSOL Multiphysics software is used to calculate the electric field distribution of the ball-plate electrode model in Figure 9a. The electric field calculation result is shown in Figure 9b, where the plate electrode is used as the ground electrode. According to the simulation results, the maximum field strength and the average field strength of the electric field are obtained. The calculated electric field unevenness coefficient $f = 1.12$, which satisfies the definition of slightly uneven field ($f < 2$).

Before the test, the gas chamber was evacuated to -0.1000 MPa and filled with N₂ (purity: 99.999%), and then evacuated again. Next, according to the proportion of each gas in the gas mixture (3.33/20/76.67%), O₂ (purity 99.999%), HFO (purity 99.5%), and N₂ are injected into the gas chamber successively. After the inflation is completed, the experimental cavity is left to stand for 12 h to fully mix the gas. After ensuring that the cavity is well sealed, subsequent operations were carried out.

In the experiment, a DC ramp voltage at an increased rate of 0.5 kV/s was applied until breakdown occurred to obtain the breakdown voltage of the HFO–N₂–O₂ gas mixture under a negative DC voltage. Through preliminary experiments, it was found that when the gas pressure is relatively low, the corona discharge phenomenon of the ball electrode after multiple breakdowns is relatively strong, which makes it difficult to obtain the breakdown voltage. Therefore, for the HFO–N₂–O₂ gas mixture with pressures of 0.1 and 0.15 MPa, 10

consecutive breakdown tests were performed. For the gas mixture at pressures of 0.2 and 0.25 MPa, 20 breakdown tests were carried out. In the continuous breakdown test, a breakdown is performed every 3 min. To quantitatively compare the influence of O₂ on the generation of HFO solid decomposition products, a thin copper sheet (with a thickness of 0.5 mm) was placed on the plate electrode. The conductive glue was used to ensure reliable conduction between the copper sheet and the plate electrode. To avoid the residual conductive glue affecting the weighing result of solid precipitates, absolute ethanol was used to wipe off the conductive glue before weighing. The analytical balance ME104/02 (measurement accuracy 0.0001 g) was used to measure the weight change of the copper sheet before and after the breakdown test.

■ ASSOCIATED CONTENT

Supporting Information

The Supporting Information is available free of charge at <https://pubs.acs.org/doi/10.1021/acsomega.1c03020>.

ReaxFF simulation results for the HFO–N₂–O₂ system; the surface state of the ball electrode after continuous breakdown test; and detailed parameters of the simulation systems (PDF)

■ AUTHOR INFORMATION

Corresponding Author

Qingmin Li – State Key Laboratory of Alternate Electrical Power System with Renewable Energy Sources, North China Electric Power University, Beijing 102206, China; orcid.org/0000-0001-5049-3980; Email: lqmee@ncepu.edu.cn

Authors

Heng Liu – State Key Laboratory of Alternate Electrical Power System with Renewable Energy Sources, North China Electric Power University, Beijing 102206, China

Jingrui Wang – State Key Laboratory of Alternate Electrical Power System with Renewable Energy Sources, North China Electric Power University, Beijing 102206, China; orcid.org/0000-0002-1160-717X

Yuheng Jiang – School of Electrical and Electronic Engineering, North China Electric Power University, Beijing 102206, China

A. Manu Haddad – Advanced High Voltage Engineering Research Centre, Cardiff University, Cardiff, Wales CF24 3AA, United Kingdom

Complete contact information is available at: <https://pubs.acs.org/doi/10.1021/acsomega.1c03020>

Notes

The authors declare no competing financial interest.

■ ACKNOWLEDGMENTS

The authors are grateful to the National Natural Science Foundation of China (Grant Nos. 51737005, 51929701, and 52081330507) and the Beijing Natural Science Foundation (3202031).

■ REFERENCES

(1) Chu, F. Y. SF₆ Decomposition in Gas-Insulated Equipment. *IEEE Trans. Electr. Insul.* **1986**, *EI-21*, 693–725.

- (2) Rabie, M.; Franck, C. M. Assessment of Eco-Friendly Gases for Electrical Insulation to Replace the Most Potent Industrial Greenhouse Gas SF₆. *Environ. Sci. Technol.* **2018**, *52*, 369–380.
- (3) Reilly, J.; Prinn, R.; Harnisch, J.; Fitzmaurice, J.; Jacoby, H.; Kicklighter, D.; Melillo, J.; Stone, P.; Sokolov, A.; Wang, C. Multi-Gas Assessment of the Kyoto Protocol. *Nature* **1999**, *401*, 549–555.
- (4) Mishra, A.; Basu, S.; Shetti, N. P.; Reddy, K. R. Metal Oxide Nanohybrids-Based Low-Temperature Sensors for NO₂ Detection: A Short Review. *J. Mater. Sci. Mater. Electron.* **2019**, *30*, 8160–8170.
- (5) Mishra, A.; Mehta, A.; Basu, S. Clay Supported TiO₂ Nanoparticles for Photocatalytic Degradation of Environmental Pollutants: A Review. *J. Environ. Chem. Eng.* **2018**, *6*, 6088–6107.
- (6) Yamamoto, O.; Takuma, T.; Hamada, S.; Yamakawa, Y.; Yashima, M. Applying a Gas Mixture Containing C-C₄F₈ as an Insulation Medium. *IEEE Trans. Dielectr. Electr. Insul.* **2001**, *8*, 1075–1081.
- (7) Chen, L.; Widger, P.; Kamarudin, M. S.; Griffiths, H.; Haddad, A. CF₃I Gas Mixtures: Breakdown Characteristics and Potential for Electrical Insulation. *IEEE Trans. Power Delivery* **2017**, *32*, 1089–1097.
- (8) Hyrenbach, M.; Zache, S. *Alternative Insulation Gas for Medium-Voltage Switchgear*, 2016 Petroleum and Chemical Industry Conference Europe (PCIC Europe), IEEE, Berlin, 2016; pp 1–9.
- (9) Preve, C.; Piccoz, D.; Maladen, R. Application of HFO1234ZEE in MV Switchgear AS SF₆ Alternative Gas. *CIREC - Open Access Proc. J.* **2017**, *2017*, 42–45.
- (10) Jia, Z.; Chen, Q.; Lin, L.; Wang, X. Study of Partial Discharge Characteristics in HFO-1234ze(E)/N₂ Mixtures. *Plasma Sci. Technol.* **2020**, *22*, No. 115403.
- (11) Calm, J. M.; Hourahan, G.; Calm, J. M. *Physical, Safety, and Environmental Data for Current And Alternative Refrigerants*, Proceedings for the 23rd International Congress of Refrigeration, International Institute of Refrigeration (IIR), Prague, 2011.
- (12) An, B.; Yang, F.; Duan, Y.; Yang, Z. Measurements and New Vapor Pressure Correlation for HFO-1234ze(E). *J. Chem. Eng. Data* **2017**, *62*, 328–332.
- (13) Lin, L.; Chen, Q.; Wang, X.; Zhang, H.; Jia, Z.; Zhang, C. Study on the Decomposition Mechanism of the HFO1234zeE/N₂ Gas Mixture. *IEEE Trans. Plasma Sci.* **2020**, *48*, 1130–1137.
- (14) Lesaint, O.; Bonifaci, N.; Merini, H.; Maladen, R.; Gentils, F. A Study of Breakdown Properties of HFO Gas under DC and Impulse Voltage, 2018 IEEE Conference on Electrical Insulation and Dielectric Phenomena (CEIDP), IEEE, Cancun, 2018; pp 606–609.
- (15) van Duin, A. C. T.; Dasgupta, S.; Lorant, F.; Goddard, W. A. ReaxFF: A Reactive Force Field for Hydrocarbons. *J. Phys. Chem. A* **2001**, *105*, 9396–9409.
- (16) Li, Y.; Zhang, X.; Xiao, S.; Chen, Q.; Wang, D. Decomposition Characteristics of C₅F₁₀O/Air Mixture as Substitutes for SF₆ to Reduce Global Warming. *J. Fluorine Chem.* **2018**, *208*, 65–72.
- (17) Zhang, X.; Li, Y.; Chen, D.; Xiao, S.; Tian, S.; Tang, J.; Zhuo, R. Reactive Molecular Dynamics Study of the Decomposition Mechanism of the Environmentally Friendly Insulating Medium C₃F₇CN. *RSC Adv.* **2017**, *7*, 50663–50671.
- (18) Li, Y.; Zhang, X.; Chen, Q.; Zhang, J.; Li, Y.; Xiao, S.; Tang, J. Influence of Oxygen on Dielectric and Decomposition Properties of C₄F₇N-N₂-O₂ Mixture. *IEEE Trans. Dielectr. Electr. Insul.* **2019**, *26*, 1279–1286.
- (19) Liu, H.; Wang, J.; Wang, J.; Hu, Q.; Chang, Y.; Li, Q. Study on Pyrolysis Characteristics of SF₆ in a Trace-Oxygen (O-2) Environment: ReaxFF(SFO) Force Field Optimization and Reactive Molecular Dynamics Simulation. *ACS Omega* **2020**, *5*, 26518–26526.
- (20) Huo, E.; Liu, C.; Xu, X.; Li, Q.; Dang, C. A ReaxFF-Based Molecular Dynamics Study of the Oxidation Decomposition Mechanism of HFO-1336mzz(Z). *Int. J. Refrig.* **2018**, *93*, 249–258.
- (21) Pu, Y.; Liu, C.; Li, Q.; Xu, X.; Huo, E. Pyrolysis Mechanism of HFO-1234yf with R32 by ReaxFF MD and DFT Method. *Int. J. Refrig.* **2020**, *109*, 82–91.
- (22) Wang, J.; Li, Q.; Liu, H.; Huang, X.; Wang, J. Theoretical and Experimental Investigation on Decomposition Mechanism of Eco-Friendly Insulation Gas HFO1234zeE. *J. Mol. Graphics Modell.* **2020**, *100*, No. 107671.
- (23) Orekhov, N.; Ostroumova, G.; Stegailov, V. High Temperature Pure Carbon Nanoparticle Formation: Validation of AIREBO and ReaxFF Reactive Molecular Dynamics. *Carbon* **2020**, *170*, 606–620.
- (24) Kashinski, D. O.; Chase, G. M.; Nelson, R. G.; Di Nallo, O. E.; Scales, A. N.; VanderLey, D. L.; Byrd, E. F. C. Harmonic Vibrational Frequencies: Approximate Global Scaling Factors for TPSS, M06, and M11 Functional Families Using Several Common Basis Sets. *J. Phys. Chem. A* **2017**, *121*, 2265–2273.
- (25) Navarini, W.; Venturini, F.; Tortelli, V.; Basak, S.; Pimparkar, K. P.; Adamo, A.; Jensen, K. F. Direct Fluorination of Carbon Monoxide in Microreactors. *J. Fluorine Chem.* **2012**, *142*, 19–23.
- (26) Huygh, S.; Bogaerts, A.; van Duin, A. C. T.; Neyts, E. C. Development of a ReaxFF Reactive Force Field for Intrinsic Point Defects in Titanium Dioxide. *Comput. Mater. Sci.* **2014**, *95*, 579–591.
- (27) Macpherson, R. W.; Wilson, M. P.; MacGregor, S. J.; Timoshkin, I. V.; Given, M. J.; Wang, T. Characterization and Statistical Analysis of Breakdown Data for a Corona-Stabilized Switch in Environmentally Friendly Gas Mixtures. *IEEE Trans. Plasma Sci.* **2018**, *46*, 3557–3565.